OTC-26286-MS

Real Time Radius of Curvature Measurement During DVC Operations Based on Flexible Pipe 3D Reconstruction

I.H. F. Santos, E. Vardaro, E. Goes, V.S. Lopes, A. Vaillant, A. Palmeiro, Petrobras; J. Kelner, V.M. Cesar, S. Pessoa, B. Reis, UFPE

This paper was prepared for presentation at the Offshore Technology Conference Brasil held in Rio de Janeiro, Brazil, 27–29 October 2015.

Abstract

When performing a direct vertical connection (DVC), the gooseneck may suffer severe damage due to the transfer of the load acting on the flexible pipe to the VCM (vertical Connection Module) when the bend restrictor is locked. On the other hand, the bend restrictor is necessary to guarantee that the minimum bend radius (MBR) of the flexible pipe is not violated during the installation.

Nowadays there is no way to assess this information in real time, except visually, thus the operation is very dependent on the pipe-laying engineer experience. In critical situations, to mitigate risks, a team of specialists onshore is requested to carefully evaluate the situation, assessing the radius of curvature, running DVC simulations using as input the geometric properties of the line and the VCM. Those geometric properties are estimated from images acquired by a remotely operated vehicle (ROV). This process is exhausting and time consuming, reducing the overall efficiency and increasing operational costs. Furthermore, it is error-prone because it does not consider the perspective effects of the image projection and the distortion caused by wide-angle lenses.

This paper describes a methodology to help the pipe-laying engineer carry out the DVC operations in a safe way. It is based on a computer vision system, SOIS, to estimate the curvature of flexible pipes during DVC operations, in order to increase the operational efficiency, through the use of stereo rig cameras and some markers along the pipe. It is faster and has a lesser margin of error than the simulated and manual assessment. This system relies on a stereo rig of lowlight cameras and on an interleaved pattern of black and white markers painted over the pipe. The 3D reconstruction process takes into account radial and perspective distortions of the images, resulting in a more accurate 3D geometry of the pipe. The system accomplishes its task through a sequence of three distinct phases: calibration, detection, and estimation of radius of curvature.

The camera calibration process, conceived for the underwater scenario, allows us to remove the radial lens distortion and to identify the camera intrinsic parameters, necessary to map image coordinates into world coordinates. The proposed detection algorithm is robust to non-uniform illumination and occlusion effects caused by fishes and particles floating around. From the detected points in both cameras of the stereo rig, it is possible to reconstruct the 3D geometry of the pipe. The estimation of the radius of curvature is obtained by fitting a 3D version of a catenary curve through the reconstructed geometry of the pipe.

Experiments demonstrated that the radius of curvature estimate is within a 3% margin of error at the 90% level of confidence. Field experiments showed that the pipe can be detected up to a distance of 15 meters. It is foreseen that the new methodology will significantly improve operational safety and shorten the average time of DVC operations, thus reducing its costs. Ongoing activities include improvements in the calibration phase to make it easier to be performed, and usability studies that are being conducted to improve the user experience with the system, especially for non-specialists in computer vision techniques.

Keywords
Direct vertical connection, radius of curvature, 3D reconstruction, camera calibration, 3D curve fitting.

Introduction

The exploitation of oil fields in Brazil's offshore has been performed using flexible pipes to make the interconnection between wells, subsea equipment (Manifolds and PLETs) and platforms, for the drainage of the production and exportation of oil and gas. Flexible pipes used for oil and gas are composed by cylindrical plastic layers and helical metallic layers, giving high flexibility to the pipe [1]. This characteristic enables the pipe to change its geometric configuration significantly. However, there is a minimum limit for the radius of curvature, defined by the pipe's manufacturer, to avoid pipe damage.

The potential failure mechanisms [2] when the minimum curvature radius is not respected are:

- Collapse of carcass, of the pressure armour or the internal pressure sheath;
- Rupture of internal pressure sheath;
- Unlocking of interlocked pressure armour layer;
- Rupture of external sheath.

Thus, the curvature radius is an important parameter that must be monitored during the pipe installation.

The installation process of a flexible pipe is divided in three phases: (i) connection with the subsea equipment at the bottom; (ii) launching the pipe on the seabed; and (iii) connection at the platform. The order in which these phases happen defines if the installation procedure is nominated first or second extremity. In the first extremity procedure, the connection of the pipe with the subsea equipment is done first, followed by the pipe laying and the pull-in at the platform. On the other hand, in the second extremity procedure the pull-in at the platform is done first, followed by the laying of the pipe and the connection to the subsea equipment. In this procedure, the pipe configuration must be adjusted to shape as a hog using floaters along the pipe or by lifting the pipe by a cable.

The connection of the pipe with the subsea equipment is critical, mainly in deep waters. Since the beginning of the use of flexible pipes in Campos Basin, in the 80s, the connection system between the flexible pipe and the equipment at the bottom has been modified due to the increase of water depth, where diving is not possible, and due to cost efficient improvements in the connection process [3], [4]. Therefore, Petrobras has modified its subsea connection system from pull-in diverless, lay-away method, Vertical Connection Module (VCM) with temporary abandonment base [5], VCM with flowline mandrel to finally VCM with Direct Vertical Connection (DVC), adopted since 1995. DVC operation is done using a VCM that consists of a gooseneck (a rigid curved pipe) with an angle of 45 to 60 degrees relating to the vertical axis. The flexible pipe is connected in one end, while in the other end, a connector is prepared to connect with the subsea resident equipment.

The connection of the end-fitting with the VCM is carried out at the working deck of the PLSV where the bend restrictor is also assembled. The bend restrictor is an attachment that protects the flexible pipe. It consists of interlocked rings that lock at a specified minimum curvature radius. The VCM has also a

shackle for uplift where a steel cable of the winch or crane of the PLSV is connected during installation. The VCM must be aligned in a vertical position in order to properly couple into the subsea equipment and also locking the connection. Figure 1 shows a sketch of the VCM in the vertical position for the first and second extremity installation procedures.

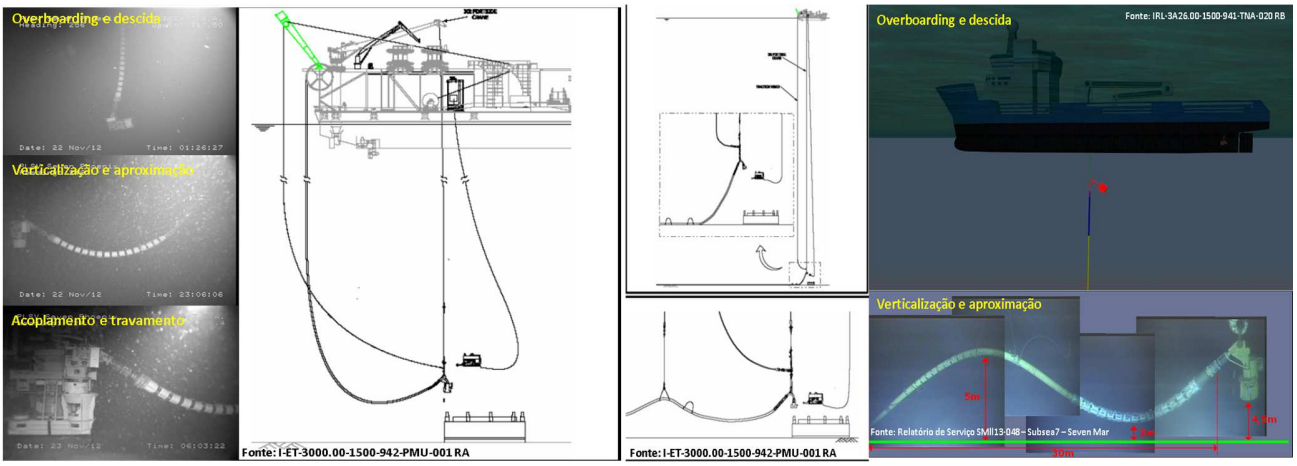

Figure 1 first extremity connection procedure (left) second extremity connection procedure (right)

The loads on the VCM are function of the geometry of the pipe and in some situations during installation it can achieve high values. To avoid transferring any possible overload imposed to the pipe directly to the subsea equipment, the VCM is designed to have a weak point of rupture. Also, after succeeding with the VCM coupling, it might be necessary to make some adjustments on the flexible line due to inability of the VCM to lock on resident equipment because of resulting loads of the line or guidance project limitation. Therefore, in order to prevent any damage to the subsea equipment due to overload or impact during the coupling, the pipelay engineer shall carefully control the radius of curvature and the vertical movement (heave) of the VCM.

Currently, the vertical connection operation is carried out by the pipe-laying engineer based on his experience in inferring the curvature radius and the vertical motion of the VCM from images transmitted by the ROV without any real-time record of those parameters. In critical situations, when it is impossible to lock the connector to the hub or when the actual pipe configuration is different from the simulated one, the operation must be interrupted and onshore support must be requested to perform numerical simulations to determine the necessary adjustments in the pipe configuration to guarantee a safety connection. This increases the installation time up to 8 hours.

Furthermore, for the onshore numerical simulations there are additional difficulties, such as image distortions caused by the cameras' lens and shooting angle. The effect of the current acting on the flexible pipe can only be considered roughly in the numerical simulations since the current profile is not completely known during the operation.

In addition, it is important to note that VCM launch and recovery operations with ROV take a long time in regions such as the Pre-salt fields, in Santos Basin, where the water depth is greater than 2000 meters. Besides that, the high pressure, temperature and the contaminants in the fluid conveyed requires the assembly of stiffer pipes, which implies in greater limit of the radius of curvature, imposing higher load on the VCM, forcing sometimes the use of floaters, even for first extremity connection. Moreover there is at least one intermediate connection hence it takes more time if a recovery becomes necessary. Thus, a system that is able to monitor the radius of curvature in real time reduces the risks of the connection operation and avoids the recovery of the VCM to surface.

The following sections describe the proposed methodology to help the pipe-laying engineer to carry out the DVC operations in a safe way providing a method for estimating, in real time, the radius of curvature along the flowline and the heave of the VCM. In this way, the pipe-laying engineer can

constantly monitor these parameters and, in critical situations, can avoid the interruption of the operation increasing its efficiency and safety. Besides that, the inaccuracies due to distortions of the cameras and due to the perspective errors associated to the recorded images by ROV, are corrected in the proposed reconstruction process.

Related Work

The capture of point position from images has already been applied in the air to determine experimentally the minimum curvature radius of flexible pipes [6] using the Qualisys® Motion Capture System, composed by four special stereoscopic cameras and with a tracking and image processing dedicated software. Reflexive marks were distributed along the pipe sample and on the connectors. The system is able to determine the Cartesian coordinates of each marker at very high sampling rate and high resolution. The sample is bent to form an arch by tensioning a cable linking the connectors. For each tension level the tracked marker positions determine the arch plane are fitted with a polynomial from which the curvature is calculated. Also in water, in laboratory experiments, to study the vortex induced vibration for risers in catenary [7], the Qualisys® system was used to accurately measure the trajectories of reflexive targets installed along the riser model. This direct measurement of Cartesian coordinates is preferable than an indirect method using strain gages and accelerometers.

The design of the 3D Submarine Dimension System and its experimental test is presented in [8]. The purpose of the system was to allow, in real time, the 3D stereo visualization and measurement of submarine structures (pipes, umbilical, connectors and valves) and anomalies. Basically, the system is characterized by an optimized hardware-and-software co-design procedure. The software includes a stereophotogrametry algorithm for precise, real-time, inspection and dimensioning operations. From a pair of cameras positioned on a ROV (Remotely Operated Vehicle), the system allows the telepresence sensation by three-dimensional vision of remote sites considerably reducing the time and, consequently, the costs of operation. The work also presents test results: laboratory small scale tests, test at PETROBRAS tank and a full-scale test on an inspection boat, with dimension of real pipe damages at Campos Basin. The system provides three-dimensional images of submarine structures allowing the acquisition of consistent and accurate data to assist the decision for the need of repairing operations.

Camera calibration is a standard procedure required in any computer vision system. Therefore, several techniques have been developed to better solve this problem, such as [9], [10], [11], and [12]. The works of Zhang [11] and Bouget [12] were used as a basis for the technique developed in this work. Regarding stereo calibration, since two cameras are required to reconstruct a flexible pipe, the works of Hu [13] is of great importance. On top of that, there is the particularity of the water being the environmental medium of application, which is dealt by the works of [14], [15], [16], [17], [18], and [19]. From these, the work of Lavest [15] is of major importance.

As for the detection phase, there are a few works about pipe detection, such as [20], [21], [22], and [23]. However, although their approaches are different from each other, all of them expect the pipe to be parallel to the optical axis of the camera, which enables the detection through the discovery of two parallel lines (representing the boundaries of the pipe). Therefore, these approaches are not appropriate to the problem addressed in this work. Concerning the binarization phase, it requires a technique that is robust to uneven illumination, but most importantly, that separates each white mark consistently and uniformly. Global techniques, such as Otsu's algorithm [24], are not appropriate, because the uneven illumination causes the failure to detect part of the pipe. Locally adaptive techniques, such as [25], [26], and [27] are generally robust to uneven illumination, but suffer from issues like: connection between segmented regions; noise in the regions surrounding the pipe; and holes inside the segmented regions.

Tracking pipes goes along the line of detection pipes, with few related solution. The work of Chua and Rizal [28] makes use of morphological operations to extract the image contours, which are regarded as subjective uncertainties that are input to a fuzzy inference system. The pipe position is detected and

steering commands are sent to AUVs. Ortiz et al. [22] uses Kalman Filter to temporally follow the pipe in a reduced search space, however under the assumption that the pipe is parallel to the camera optical axis. The reconstruction of primitives has already been investigated in [29], [30], [31], [32], [33], [34] and [35], from which the work of Xiao and Li [35] are the most influential to this one, given its method of simultaneously fitting a rational B-spline to each of the stereo samples.

In the following section we present the 3D reconstruction pipeline process to reconstruct the flexible pipe 3D geometry during DCV connections.

The Flexible Pipe 3D Reconstruction Methodology

In order to detect and reconstruct the 3D geometry of flexibles pipes, the proposed methodology relies on an interleaved pattern of marks, which should cover all the surface of the segment of pipe being analyzed. This pattern enables the system to distinguish segments of pipe along the time.

Once calibrated, the system continuously attempts to identify the interleaved pattern in the images. The detection algorithm uses topological constraints to segment the image into the best possible candidates for the white marks, and then applies the backtracking technique to choose from these candidates which ones actually belong to the pipe.

Since the detection process takes a long time to process, due to the need to search the whole image, a different approach is used to follow the pipe along the time. The tracking procedure is a two-step energy maximization technique based on the fact that the pipe only moves slightly from frame to frame, thus narrowing the search range.

Upon finding the pipe in each image separately, the 3D geometry of the pipe medial axis is reconstructed as a curve, by simultaneously fitting a curve to the set of points from each image. At last, a catenary curve is fitted to the projection of 3D point on the dominant plane sampled from the curve, in order to assess the pipe's curvature. The whole system is described in details in the following sections.

Calibration

The camera calibration is the process used to determine the intrinsic and extrinsic parameters of the camera on a world coordinate system [36]. It is important to get an accurate calibration because computer vision algorithms that perform dense reconstruction, visual inspection and location of objects need precise information to make it possible to match the real world (three-dimensional) data to the image (two-dimensional) [37]. When two cameras are used, stereo calibration is required to determine their relative position.

The proposed calibration process averages the poses obtained at each point of view on the calibration footage, as described in [38], and further refines the results using the Levenberg-Marquardt algorithm to minimize the reprojection error. The cameras are independently calibrated using a tridimensional pattern, and because of the distance between the stereo cameras, a double pattern was used to calibrate the stereo rig, as proposed in [13]. The calibration is performed using an OpenCV function based on the algorithms described in [11] and [12].

Pipe detection

Offshore operations usually take place in deep underwater environments that lack natural illumination, making the only light sources available those ones attached to the ROV. ROVs are also equipped with special underwater cameras systems, which can capture images in low light conditions (10^{-3} lux). These images are monochromatic, low resolution (usually NTSC or PAL standards), and tend to be blurred due to the underwater light scattering, rendering the scenario less than ideal for computer vision applications. In order to be robust to the low quality of the images, the proposed

technique relies on an alternating black and white (a vertebra) regions painted over the pipe. Since the region of the pipe which is to be monitored is relatively short, this manual task is affordable. The proposed detection technique is divided into three stages: a pre-processing stage to reduce image noise; a binarization stage to find the vertebrae candidates; and a searching stage to identify which of the candidates are actual vertebrae. Each phase is further explained in the following subsections.

Pre-processing

The images captured by the ROV cameras are subject to a great amount of noise, such as particles and fish. Therefore, in order to reduce the influence of these artifacts, two blurring filters are used before the binarization of the images. First, a bilateral filter [39] is used to remove small particles floating around, while preserving the vertebrae edges. Finally, a Gaussian filter is used to uniformly smooth the images.

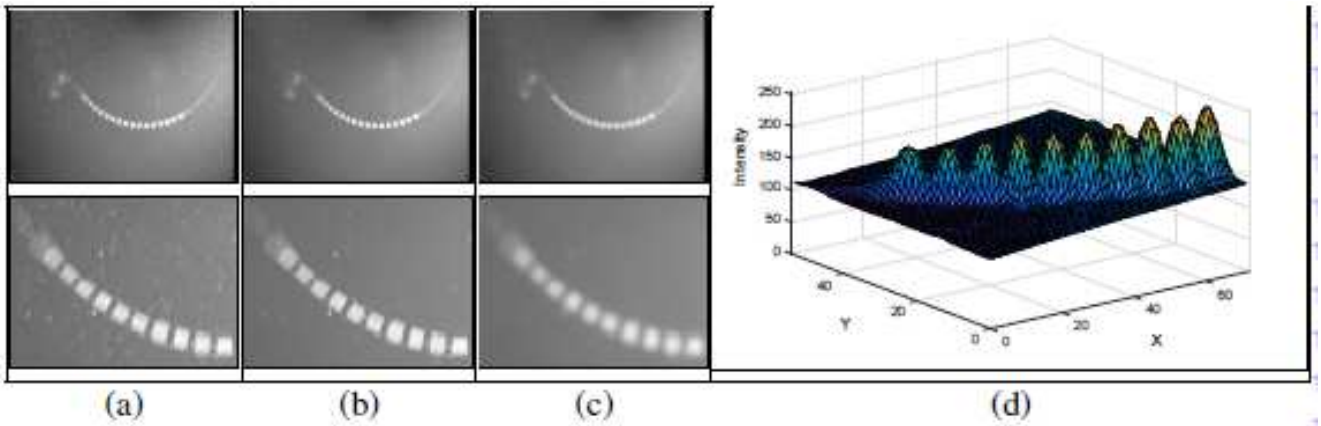

Figure 2 Pre-processing and binarization steps of the detection technique, where (a) presents the input image, (b) presents the result of the bilateral filter, (c) presents the result of the Gaussian filter, and (d) presents the result image as a surface plot.

Binarization

The binarization technique takes into account the topology of the intensity of the pixels to filter the white regions. It was conceived in order to be robust to non-uniform illumination, which is important due to the scattered light rays in underwater environments, and to separate each white region into their own blob, even if there is only a shallow valley of intensity between two bright regions.

The idea behind the technique consists in finding peaks in the pre-processed image. Observe that, whenever a pipe bright mark appears in the image, it will produce a peak (Figure 2d), since these are solid white regions with a dark vicinity smoothed by the Gaussian filter. So, by gathering every peak from the pre-processed image, all the white marks will be found. While this approach will generate much false positive detection, due to particles floating around, the most important feature is to avoid false negatives, since the false positives will be handled later. Given that the marks come from solid white regions, it is expected that they will not present any holes. Therefore, any mark containing one or more holes is filtered out. The result of this topological binarization technique is a binary image where every potential region is marked in white, and a set of blobs.

Segmentation

Some of the blobs found in the binarization step are related to floating particles and other equipment present in the scene. Thus, one has to find out which blobs in this set are actually due to the pipe vertebrae. This is achieved by searching for the longest chain of blobs that respect restrictions inherent to a pipe, i.e. distance between vertebrae, the length of the gap between vertebrae (black regions) and the

length of the radius of a blob representing a vertebra. This chain is represented by a sequence $V = \{j_k\}_{k=1}^{m} = j_1, j_2, \dots, j_m$, where j_k is the index of a blob b_i (i.e. $j_k = i$). A backtracking algorithm finds the sequence V. It starts by iterating over all blobs of B. For each blob visited that satisfies restrictions, its index is inserted into V. When no more viable blobs can be found, the current V is stored (if it is the longest sequence found so far) and the algorithm backtracks (i.e., it steps back by removing the last element of V). This process is repeated until all blobs are visited.

Tracking

Given that the pipe moves slowly around, due to the resistence offered by the water, it is possible to avoid searching for the pipe in the whole image by looking for it exclusively around its position in the last frame. However, since it is a flexible body, it is necessary to consider that the projection of the pipe may change heterogeneously in the image. The alternating pattern marked over the pipe enables us to compare independently different segments of the pipe between two sequential frames. This comparison is based on the hypothesis that the pipe projection is the brightest element in the image I. Thus, the tracking technique attempts to find the pipe by maximizing the intensity of a region $\mathcal{R}$, which is parametrized by the thickness of the pipe (s dimension) and by a parametric curve $\boldsymbol{x}(t)$, describing the projection of the pipe medial axis (PMA). The region $\mathcal{R}$ is defined by the function $\boldsymbol{R}(s, t, \boldsymbol{x}(t))$. The problem is summarized as finding the parametric curve $\boldsymbol{x}^*$, such that

$$\boldsymbol{x}^* = \arg\max_{\hat{\mathbf{x}}} \iint I\left(\boldsymbol{R}\left(s, t, \hat{\boldsymbol{x}}(t)\right)\right) ds\, dt.$$

Strictly solving the problem through this formulation leads to the degeneration of the curve. To mitigate this problem, the tracking is divided into a longitudinal and a transversal phase. To simplify the computation during each unidimensional phase, the image is transformed into a longitudinal and transversal parametrization, resulting in $T(s, u)$, which is based on the tracking results of the previous frame.

$$T(s, u) = \sqrt{I\left(\boldsymbol{R}(s, t)\right)}, \text{ where } u = \int_{t_{min}}^{t} \left\| \frac{d\boldsymbol{x}(\tau)}{d\tau} \right\| d\tau.$$

Longitudinal Tracking

The longitudinal tracking is responsible for identifying the position of the extremities of the pipe in the current frame along the u dimension. By defining that these points are located on bright marks of the pattern, the longitudinal tracking attempts to maximize the energy in a window around them using the Gauss-Newton method. Each extremity is handled separately by solving

$$u^* = \arg\max_{\hat{u}} \int_{\hat{u}-\frac{\omega}{2}}^{\hat{u}+\frac{\omega}{2}} \int_{0}^{1} T(s, u)^2\, ds\, du,$$

where ω is the empirically defined window size.

Transversal Tracking

Contrary to the longitudinal tracking, the transversal tracking aims at adjusting the whole curve along the s dimension. Assuming that the pipe projection is the brightest region of I, the energy inside the region $\mathcal{R}$ is maximized under the constraint that the PMA should be smoothly adjusted. This is done by a smooth function $\phi(u; \boldsymbol{q})$, governed by the parameter vector $\boldsymbol{q}$. The transversal tracking is defined then

as finding the parameter vector $\boldsymbol{q}^*$, such that

$$\boldsymbol{q}^* = \arg\max_{\hat{q}} \int_0^1 \int_{u^*_{min}}^{u^*_{max}} w(s)T(s+\phi(u;\hat{\boldsymbol{q}}),u)^2 du ds,$$

where $w(s)$ is a weighting function used to reduce the influence of bordering pixels.

Reconstruction

Once the smooth function $\phi(s;\boldsymbol{q})$ is applied to the tracked points in both images, the result is two sets of sample points $\{\boldsymbol{p}_i\}$ and $\{\boldsymbol{p}'_j\}$. The next step is to estimate the 3D curve $\boldsymbol{x}(t)$ that represents the PMA, which was achieved by simultaneously fitting a curve to each of the rectified sample points, resulting in the curves $\boldsymbol{x}(t;\{\boldsymbol{q}_k\})$ and $\boldsymbol{x}(t;\{\boldsymbol{q}'_k\})$, where $\boldsymbol{q}_k$ and $\boldsymbol{q}'_k$ are the control points of each curve. By modelling the fitting as a least-square problem, it is solved by minimizing the cost

$$\sum_i \left\|\boldsymbol{p}_i - \boldsymbol{x}(t_i;\{\boldsymbol{q}_k\})\right\|^2 + \sum_j \left\|\boldsymbol{p}'_j - \boldsymbol{x}(t_j;\{\boldsymbol{q}'_k\})\right\|^2.$$

Fitting

After the reconstruction stage, it is necessary to adjust a suitable curve to these points in order to be able to compute the curvature along the pipe. Several curve models can be fitted to the data, such as polynomial curves or parametric B-splines, and each one of them requires a specific algorithm. It also presents different matching capabilities and sensitivity to the curvature estimation.

This work makes use of the catenary curve model [40], which represents a curve described by uniformly dense, perfectly flexible and inextensible cables hanged by its endpoints. Although real pipes do not configure such a catenary due to their natural bending resistance, it is a suitable model for the experiments, given its ideal sensitivity to the curvature estimation. The parametric equation for a catenary is defined by $y(t) = a\cosh(\frac{t}{a})$, where a is the minimum radius of curvature (which is the inverse of the maximum curvature).

The process of fitting the curve to the points is a nonlinear optimization, which can be computed by the Levenberg-Marquardt optimization method. Given the parameter vector $\beta = (a, \theta, t_x, t_y)$, determining the curve's minimum radius of curvature, rotation and translation parameters, the problem can be summarized as finding

$$\beta_{optimal} = \arg\min_{\beta} \sum_i \left(\hat{y}_i - a\cosh\left(\frac{\hat{x}_i}{a}\right)\right)^2,$$

where

$$\begin{bmatrix}\hat{x}_i \\ \hat{y}_i\end{bmatrix} = \begin{bmatrix}\cos\theta & -\sin\theta \\ \sin\theta & \cos\theta\end{bmatrix}\begin{bmatrix}x_i \\ y_i\end{bmatrix} + \begin{bmatrix}t_x \\ t_y\end{bmatrix}.$$

Field Tests and Results

This section presents the tests that were conducted in the project. The first test was made in Baleia Azul field in 2012, where the main objective was to establish a proof of concept. Complementary tests were done in 2013 and 2014 at Petrobras R&D Center and at Federal University of Rio de Janeiro, respectively. The first field test with real time processing of the images was carried out in April 2015 on board of PLSV Sapura Topazio during the interconnection of the 6" production flowline of the well 7-SPH-002 to the PLET located at Sapinhoá field under 2140 meters of water depth in Santos Basin. In this operation, a first and second extremity connection was done, allowing evaluating the system

performance in both operations.

Baleia Azul field tests

A proof of concept of the method proposed in this work was executed in November 2012, in the PLSV Seven Phoenix, during the first extremity connection of the 8" production line of the well BAZ-01 under 1350 meters of water depth, located at the Baleia Azul field. Two SIT cameras installed on a ROV with a fixed distance between them have been used in this operation. The flexible pipe and its accessories bend restrictor and connector, were painted following the specified pattern aiming to mark a reference and highlight the pipe in the images. During the operation, images of the region close to the VCM were recorded. These images were processed to estimate the curvature radius afterwards.

On the proof of concept, the radius of curvature estimation of the proposed method was compared to the analysis performed with the software OrcaFlex [41]. Although the cameras were not calibrated it was possible to estimate the curvature in the pixel domain and then adjusted through a known metric distance in the image. This way it was possible to retrieve the metric curvature, which always was less than 0.04 rad/m different from numerical analysis, throughout the pipe, as shown in Figure 3.

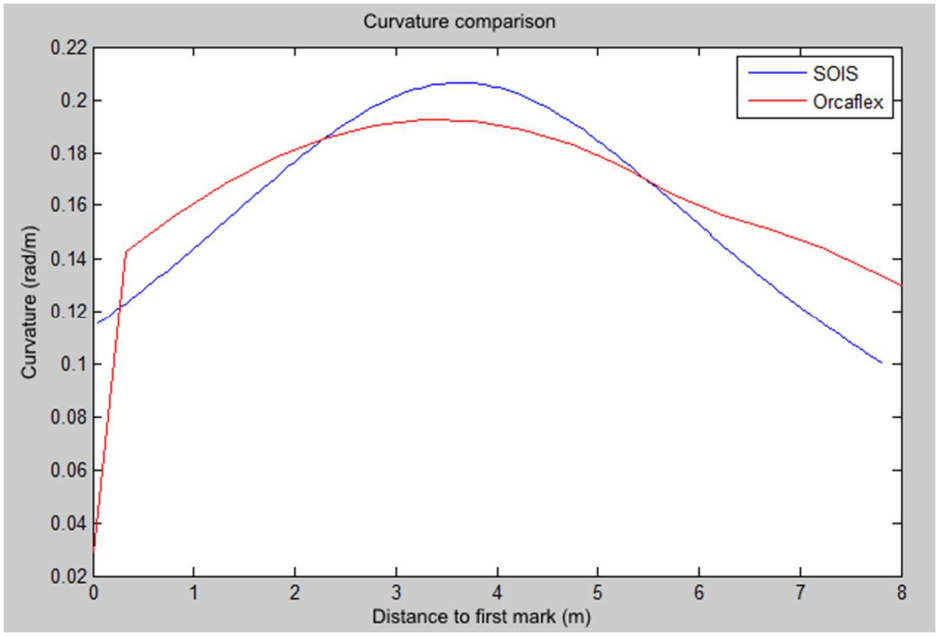

Figure 3 Comparison between Curve Reconstruction Done by SOIS and the Specialist's Analysis with OrcaFlex Software.

Petrobras Research and Development Center tests

The experiment on the laboratory of Subsea Technology Group of the Petrobras R&D Center was performed with a submerged pipe mock-up in a scale of 1:10, made of conduit filled with an iron chain, and painted with the specified pattern. Video footages where captured using two Imenco SDS1210 cameras, 83 mm apart from each other, which has a resolution of 640x480 pixels. Since the iron chain behaves approximately as a catenary curve, this curve model was used the ground-truth for the system's estimations. Nine videos were captured: 2 with a curvature radius of 48.4 cm; 5 with a curvature radius of 27.9 cm; and 2 with a curvature radius of 13.7 cm. Different positions between cameras and pipe were analyzed. The summary of this experiment is presented in Table 1.

Table 1. Summary of The Experiment At The Subsea Technology Group Of The Petrobras R&D Center Lab.

Video #	Curvature Radius	Mean Error	Standard Deviation	Maximum Error	Error (%)	% of Frames Reconstructed
1	484 mm	16.66 mm	14.02 mm	98.96 mm	3.44%	**91.99%**
2	484 mm	5.82 mm	4.62 mm	99.79 mm	1.2%	**99.57%**
3	279 mm	6.28 mm	8.53 mm	46.77 mm	2.25%	**99.68%**
4	279 mm	5.72 mm	8.12 mm	99.90 mm	2.05%	**98.52%**
5	279 mm	9.19 mm	6.42 mm	91.72 mm	3.29%	**100%**
6	279 mm	11.16 mm	1.88 mm	99.64 mm	4%	**99.48%**
7	279 mm	13.79 mm	12.39 mm	51.22 mm	4.94%	**95.71%**
8	137 mm	11.24 mm	11.73 mm	46.64 mm	9.05%	**91.17%**
9	137 mm	9.94 mm	4.46 mm	97.73 mm	7.26%	**99.80%**

The highest percentage errors were found when the curvature radius was smaller, probably because the pipe is less like a catenary curve when the curvature radius is small. Most of the video frames that were not reconstructed occurred because the pipe was not properly framed. The highest deviation occurred when the pipe was oblique to the camera, as presented in Figure 4. The errors in 7 of the 9 videos were smaller than 5%, which is around the same magnitude of the ground-truth measurement.

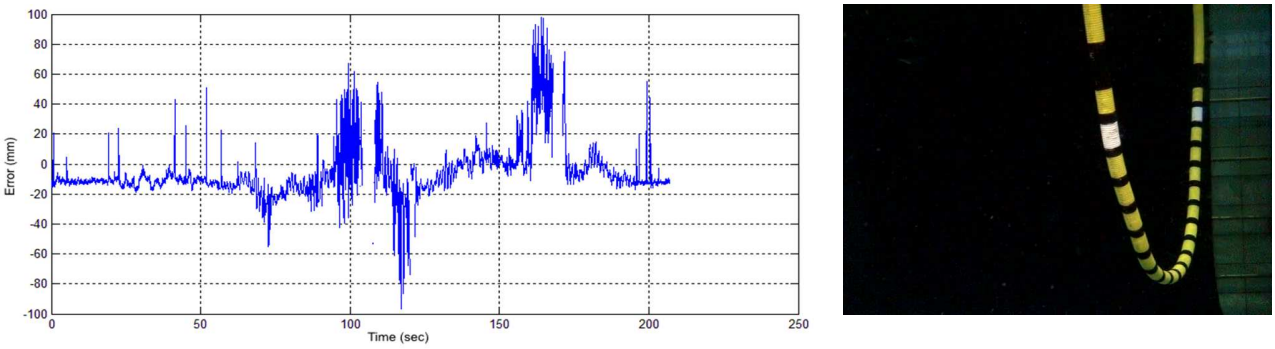

(A) (B)

Figure 4 (A) Shows the plot of the error on video 1, which presented high std. deviation around frame 100. (B) Shows a video frame of the pipe when the cameras where oblique to it

Federal University of Rio de Janeiro tests

At the Laboratory for Ocean Technology, LabOceano, of Federal University of Rio de Janeiro (UFRJ), two scenarios were tested: in air and in water. Both visual odometry, which is the process of determining the position and orientation of the camera by using only the images captured, and the radius of curvature were analyzed.

In the first scenario, in air, is compound by a hexapod, two Kongsberg OE15-101c cameras away 8.891 cm, a dark bulkhead, chain and foam. The cameras are attached to the hexapod (Figure 5a), which can perform programmed translation and rotation movements along three axis, resulting in six degrees of freedom. The chain is fastened only by its ends, conforming to the shape of a catenary curve. It is covered with foam and secured with electrical tape with regular spacing, representing a pipe on a scale of 1:9.02. It was positioned in front of the dark bulkhead (Figure 5b) to simulate the lighting conditions at great depths. The model was placed at 1.5 meter away from the camera, which is equivalent to 13.53 meters in real scale, and 18 meters if the out-of-water camera FOV is considered.

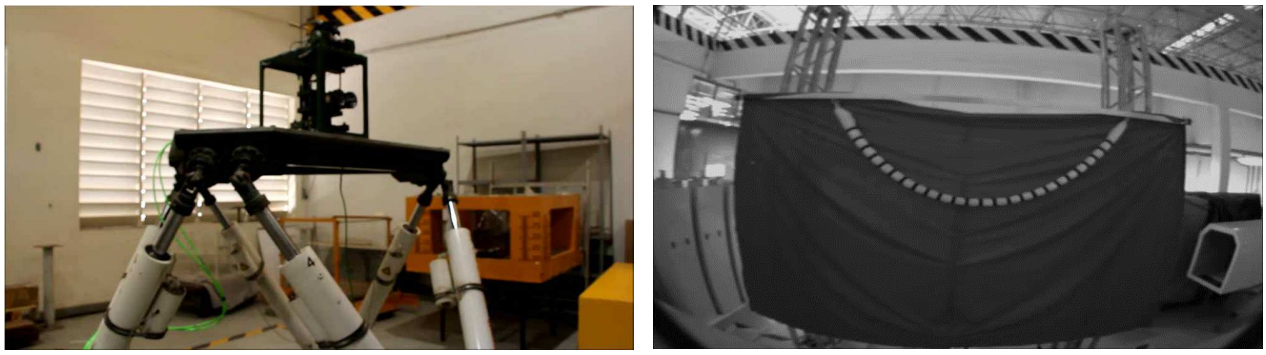

(A) (B)

Figure 5 (A) Hexapod with the stereo cameras attached. (B) Dark bulkhead with pipe made of chain and foam in front of it

Two different pipe settings were used in the experiments: pipes with curvature radius of 30 cm and 54 cm. The environment settings were designed to stress the algorithms, since the radial distortion is much bigger out of the water, the speed of the camera is faster (≈ 1 m/s) and the distance between the camera and the model is beyond the work distance (18 meters vs. 10 meters).

During the test, the camera position and orientation ground-truth is known from the movements selected in the hexapod. Those movements were compared to the visual odometry outcome. In Figure 6, the position of the camera recovered by SOIS is shown.

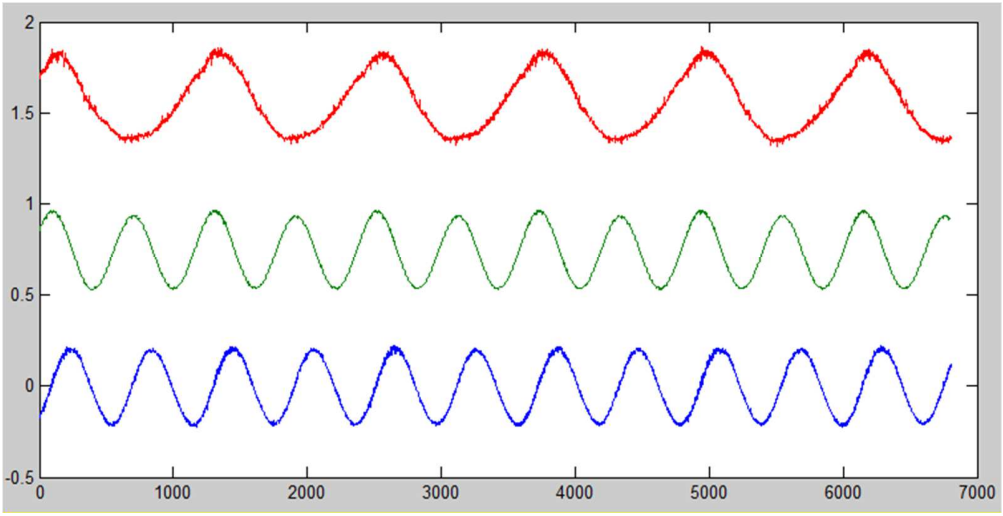

Figure 6 Translational movements along the three axis (X: Red, Y: Green, Z: Blue) recovered by SOIS

In Table **2**, the results of the analysis for various camera movements are summarized. In this table g is the curvature radius ground-truth, r_i is the curvature radius of the ith frame, $\overline{x_i}$ is the average value of x_i,
$|\overline{r_i} - g|$ is the absolute error of the average of the curvature radius, $\sigma(r_i)$ is the standard deviation of the curvature radius, $\overline{|r_i - g|}$ is the mean absolute error, $\overline{|r_i - g|/g}$ is the mean absolute percentage error, $\# < 5\%$ is the rate of frame with error less than 5%, and $\# < 10\%$ is the rate of frame with error less than 10%.

From Table **2** it is seen that SOIS performs better with the bigger curvature radius setting, which is closer to the real scenario configuration. This is due to the curve fitting adjusting a catenary curve to the pipe, which tends to form a different curve when its curvature radius is smaller. On this curvature setting, the error is consistently smaller than 10%, and even smaller than 5% on many frames. Overall, the mean absolute percentage error is smaller than 10%.

Table 2. Summary of the experiments with the hexapod in LabOceano at UFRJ.

Movement	g	$\lvert\overline{r_i} - g\rvert$	$\sigma(r_i)$	$\overline{\lvert r_i - g\rvert}$	$\overline{\lvert r_i - g\rvert / g}$	# < 5%	# < 10%
Surge	**30**	2,92	0,42	2,92	9,75	**0,97**	**51,53**
	54	3,01	0,95	3,01	5,58	**37,84**	**99,98**
Sway	**30**	2,59	0,75	2,59	8,63	**12,41**	**63,76**
	54	2,63	1,19	2,63	4,86	**47,03**	**99,94**
Heave	**30**	0,99	0,89	1,04	3,47	**72,36**	**96,67**
	54	2,61	2,02	2,83	5,25	**40,47**	**99,23**
Roll	**30**	2,79	0,41	2,79	9,28	**0,00**	**66,43**
	54	3,23	1,45	3,24	6,00	**34,91**	**96,88**
Pitch	**30**	2,60	0,85	2,60	8,67	**14,45**	**56,62**
	54	3,15	1,25	3,15	5,84	**36,85**	**97,78**
Yaw	**30**	2,64	0,57	2,64	8,79	**0,65**	**63,49**
	54	3,31	1,13	3,31	6,14	**31,36**	**97,99**
Sway + Yaw	**30**	2,69	0,71	2,69	8,96	**2,51**	**67,58**
	54	3,12	1,24	3,12	5,78	**44,91**	**99,06**
Heave + Pitch	**30**	2,77	0,87	2,77	9,23	**9,77**	**53,22**
	54	2,82	1,56	2,84	5,26	**42,09**	**97,71**
Surge + Sway + Heave	**30**	3,11	0,29	3,11	10,36	**0,00**	**34,87**
	54	3,89	0,89	3,89	7,20	**7,59**	**95,71**

The second scenario, in water, is compound by a tank, a support, two Kongsberg OE15-101c cameras placed 80 cm apart, illuminators near the cameras (30 cm), chain and foam. The tank has dimensions 40 m (length) x 30 m (width) x 15 m (depth) and has three floating bottoms that can control the depth (Figure 7). To simulate the low light condition of deep underwater, two of the bottoms were suspended to create a dark environment in the water, as can be seen on Figure 7a.

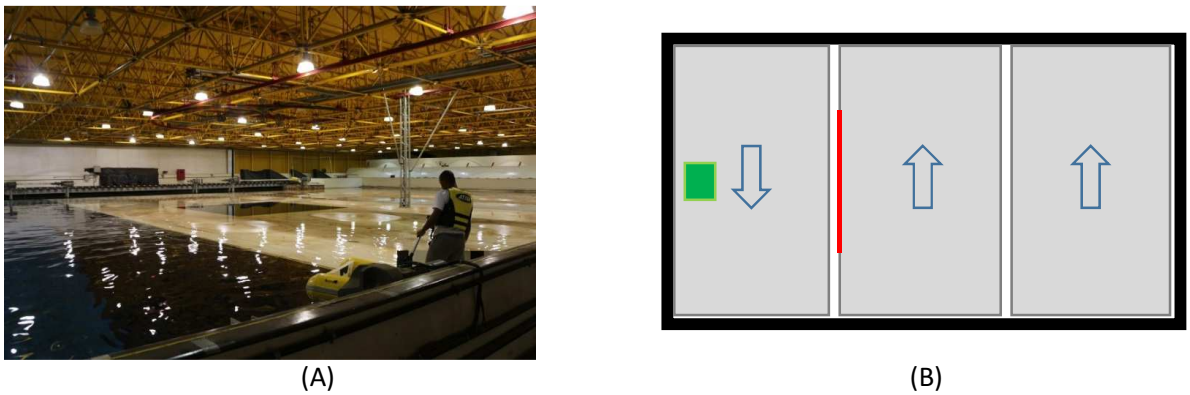

(A) (B)

Figure 7 (A) The tank with two of its bottoms floating. (B) Schematic of the tank bottom settings with the support highlighted in green and the pipe in red

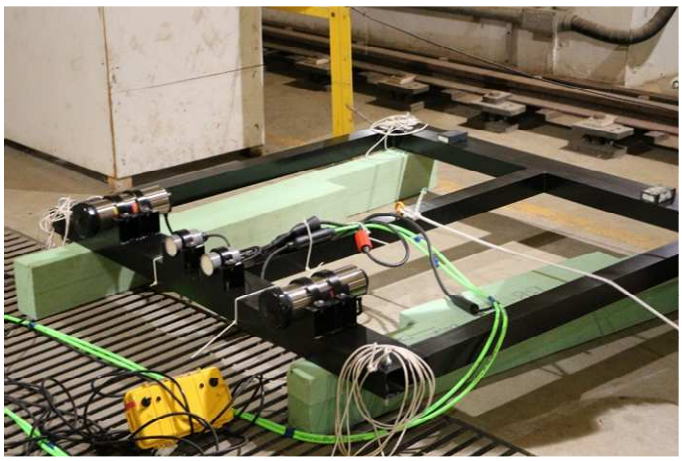

Figure 8 The support with the cameras and the illuminators attached

The laboratory lights were also turned off. The cameras and the illuminators are attached to the support (Figure 8) and the movements of the support inside the tank were carried out with the aid of ropes. The chain is covered with foam and secured with plastic tape with regular spacing to represent a pipe on a real scale. It is fastened only by its ends, configuring an upside-down catenary shape, since the foam density is much lower than the water's in this scenario. The position of the support (green) and the pipe (red) in the tank can be seen on Figure 7b.

The Figure 9a shows a sample picture of the pipe and the Figure 9b a captured video. The ground-truth radius of curvature was calculated using the distance between the ends and the length of the pipe using several methods resulting in the average value of 2.99 meters.

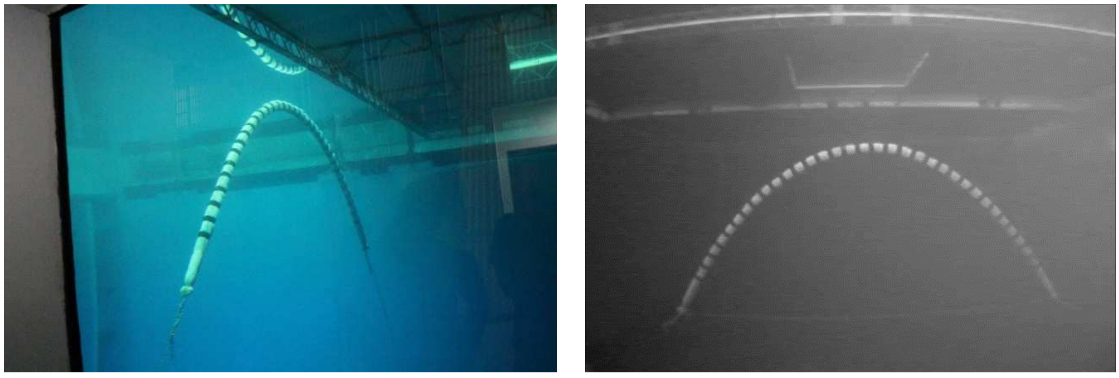

(A) (B)

Figure 9 The body of proof seen from a window on the side of the tank (A) and from the cameras (B).

Three video footages were captured: the first one is of an approximation movement, one meter at a time, ranging from 10.95m to 5.95m; the second is of a heave movement with 1 meter amplitude, and linear and slow velocity; and the last is of the same heave movement, with linear and quick velocity. During the approximation movement, when the cameras got too close to the body-of-proof, only a small region of the pipe was seen by both cameras, which caused curvature radius to be estimated incorrectly from that time onwards. As for the heave movements, the SOIS estimated consistently the curvature radius with fewer than 5% of error, achieving a mean absolute percentage error of 2.17%. Table 3 summarizes these results.

Table 3. Summary of the experiments in the basin tank in LabOceano at UFRJ.

Movement	g	$\overline{r_i}$	$\overline{r_i} - g$	$\sigma(r_i)$	$\overline{\lvert r_i - g \rvert}$	$\overline{\lvert r_i - g \rvert / g}$	# < 5%	# < 10%
Approximation	2.99	2.77	-0.21	0.216	0.24	8.13	**45.72**	**61.13**
Heave (0.02 Hz)	2.99	2.92	-0.064	0.028	0.064	2.17	**99.93**	**99.98**
Heave (0.8 Hz)	2.99	2.92	-0.063	0.027	0.063	2.12	**99.95**	**100**

Sapinhoá Field tests

For the field test in Santos Basin, two Kongsberg OE15-101c SIT cameras were used placed 80 cm apart from each other. The alternating pattern was both painted and draped with tape, in order to enforce the pattern over the bend restrictor (including anodes and slings). However, due to the harshness of the environment, the pipe was not completely covered with the pattern, as some of the tape was ripped and the paint scratched. Still, the detection phase was robust enough to overcome punctual pattern failures.

Although the cameras were calibrated, there isn't ground-truth for the curvature. A good estimation of the correctness of the system can be derived from a comparison with sonar data. By processing the sonar images in order to rectify it and then estimate the pipe localization and dominant plane, it is possible to assess whether the reconstruction phase is correct. Two analyses were done: the first one when the pipe was hanged by one end; and the second one during the load transfer. On the first one, the sonar estimated the distance to the pipe to be 8.45 m, while SOIS estimated it as 8.63 m, what results in an error of 0.18 m (2.13 % of the total distance). On the second one, it was possible to assess the dominant plane angle to the ROV, since the pipe was hanged by both ends. The sonar estimated the distance to center of the ROV to be 11.56 m and the angle to projection plane to be 46.29°, while SOIS estimated the distance to be 11.66 m and the angle, 45.79°. Thus, the angle error was 0.5°, and the distance error 0.1 m (1% of the total distance). In spite of not having ground-truth, the SOIS did estimate the curvature of the pipe, such as presented in Figure 10.

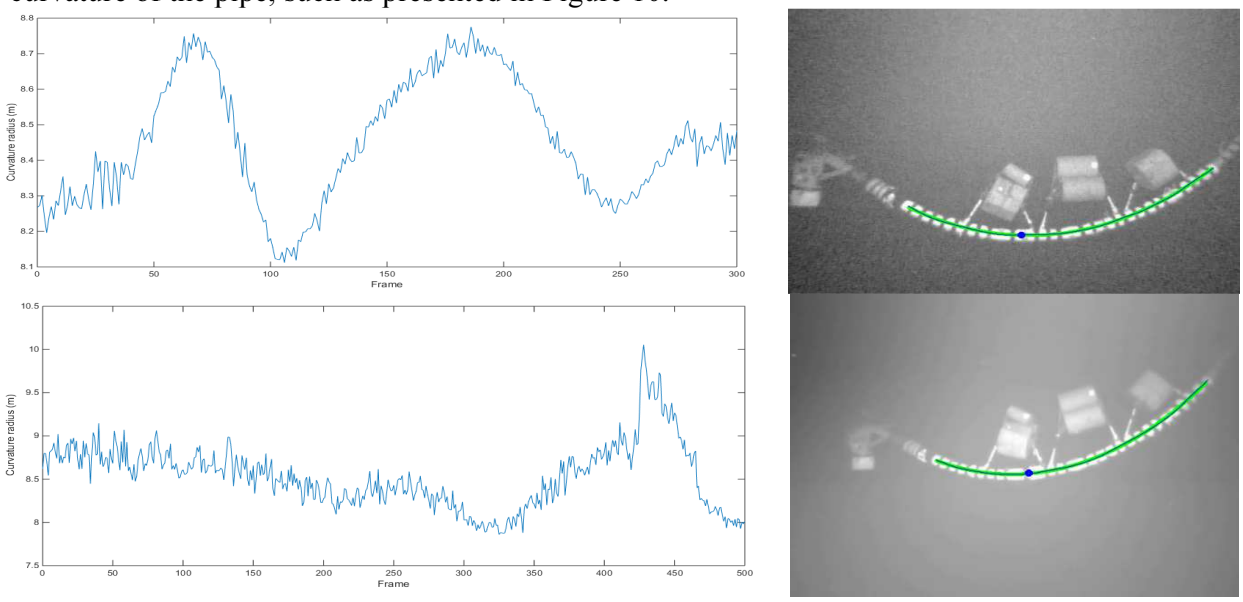

(A) (B)

Figure 10 (A) shows the plot of the curvature radius in two of the videos from the field test. (B) Shows a frame sample of the video overlaid by the reconstructed curve and the minimum curvature radius indication.

A second way to determine whether the system is accurate can be found by analyzing the reconstruction of the pipe through its projection on the image. If the projection of the reconstruction pipe (drawn in green over each image from **Figure *11***) is exactly over the center of the pipe in the images, it is highly likely that the reconstruction is accurate. In **Figure *11***, it is shown the result of the pipe reconstruction under 4 different scenarios. In every one of them, the reconstructed pipe projection lies precisely over the center of the pipe, indicating the reconstruction is correct.

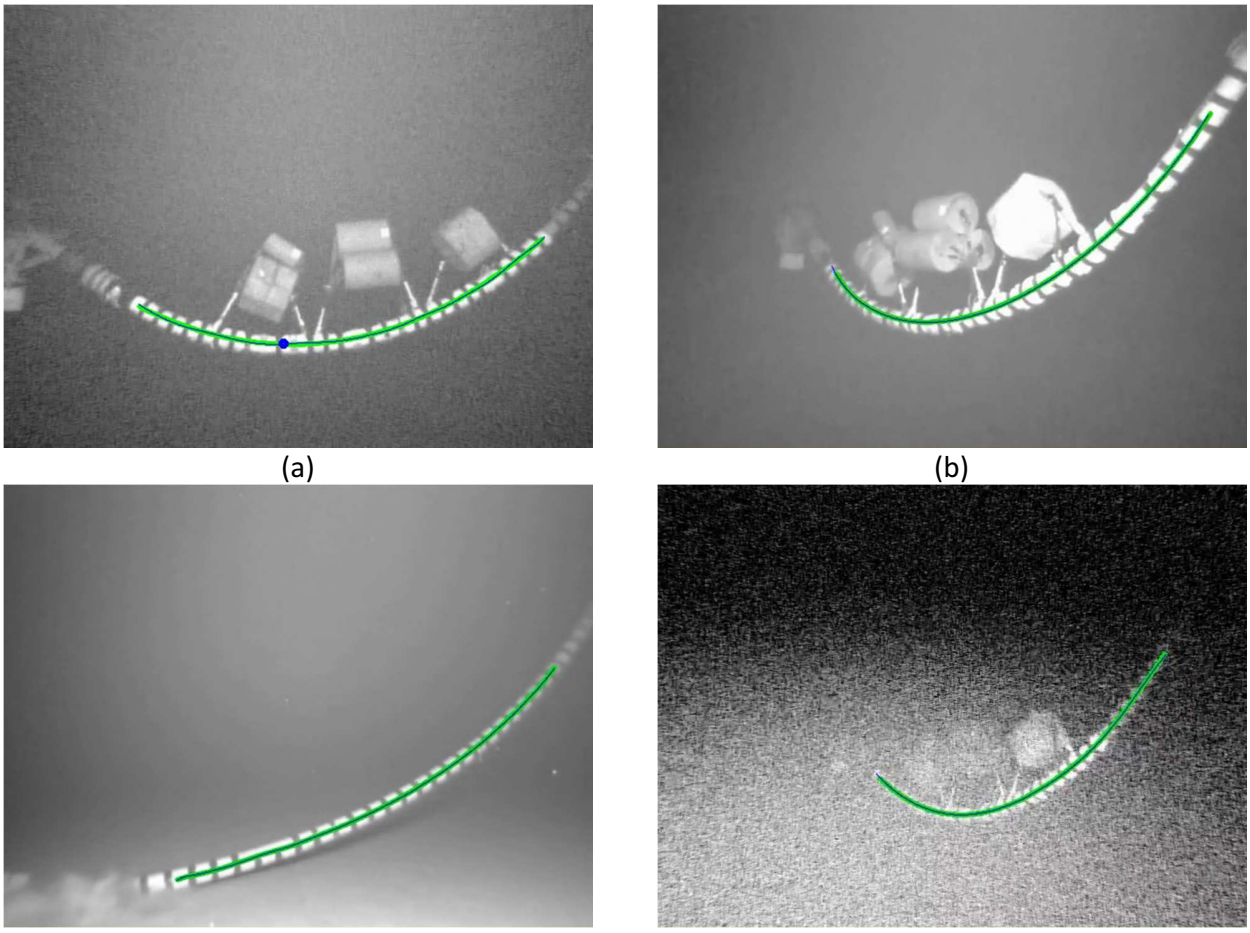

Figure 11. Pipe reconstruction under different pipe conditions, such as: (a) close to the camera; (b) oblique to the camera; (c) touching the sea floor with one end; and (d) on a heavily noised image.

Conclusions and Future Work

The tests carried out in laboratory and on the field exhibited good results, demonstrating that the methods developed for tracking, reconstruction and evaluation of the radius of curvature of the flexible pipe the results in the range of accuracy required for the installation operations of flowlines and subsea equipments. Thus, besides the tests performed so far, other field tests are planned to complete the development of the procedures and the software.

Although the method is applied for the DVC operation specifically the method can be used in other activities that have the necessity to observe the radius of curvature once the flexible pipe is marked correctly.

It is expected that the use of SOIS will increase the safety and the efficiency of the flowline connection to subsea equipments and give new possibilities for other similar operations.

Acknowledgments

Thanks to Sapura Navegação Maritima S.A. for the technical assistance in this project. The authors would also like to thank the support provided by the research funding organizations CNPQ and FAPEPE.

References

[1] J. J. Ferret e L. C. Bournazel, "Calculation of Stresses and Slip in Structural Layers of Unbounded Flexible Pipes," *Journal of Offshore Mechanics and Artic Engineering,* vol. August, 1987.

[2] American Petroleum Institute, "API Recommended Practice 17B - Recommended Practice for Flexible Pipe," API, May 2014.

[3] Moreira J.R.F. e et ali, "Further Advances in Deepwater Flowline Connection Technology," em *OTC 8239*, Houston, May 1996.

[4] M. B. Cerqueira e P. Couto, "A Vertical Connection System to Attach Flexible Pipeline to a Subsea Manifold," em *OTC-6980*, Houston,USA, 1992.

[5] L. R. P., C. A. S. Paulo e E. A. Neto, "Campos Basin - Subsea Equipment: Evolution and Next Steps," em *OTC 15223*, Houston, May 2003.

[6] R. L. Tanaka, R. T. Gonçalves e a. et, "Minimum Bending Radius (MBR) Tests of Flexible Pipes: An Experimental Approach via Optical Motion Capture and Image Processing," em *OTC Brasil*, Rio de Janeiro, October 2011.

[7] R. T. Gonçalves, A. L. C. Fujarra e a. et, "A Model Scale Experimental Investigation On Vortex-Self Induced Vibrations (Vsiv) Of Catenary Riser," em *OMAE2013 - ASME 2013 32nd International Conference on Ocean, Offshore and Arctic Engineering*, Nantes, France., 2013.

[8] L. C. P. Messina e et ali, ""Three Dimensional Imaging System for Subsea Inspection"," em *OMAE2006-92629 Proceedings of OMAE2006 25th International Conference on Offshore Mechanics and Arctic Engineering*, Hamburg, Germany, 2006.

[9] R. Tsai, "A versatile camera calibration technique for high-accuracy 3d machine vision metrology using off-the-shelf tv cameras and lenses," *Journal of Robotics and Automation,* vol. 3, nº 4, pp. 323-344, 1987.

[10] J. Heikkila e O. Silven, "A four-step camera calibration procedure with implicit image correction," em *Conference on Computer Vision and Pattern Recognition*, Washington, DC, USA, 1997.

[11] Z. Zhang, "A flexible new technique for camera calibration," *IEEE Transactions on Pattern Analysis and Machine Intelligence,* vol. 24, nº 1, pp. 1330-1334, 2000.

[12] J. Y. Bouguet, "Matlab calibration tool".

[13] X.-K. Hu, "Field calibration method for extrinsic parameters of binocular stereo camera," em *Information Engineering and Computer Science*, 2009.

[14] M. Bryant, D. Wettergreen, S. Abdallah, A. Zelinsky e E. Zelinsky, "Robust camera calibration for an autonomous underwater vehicle," em *Australian Conference of Robotics and Automation*, 2000.

[15] J. M. Lavest, G. Rives e J. T. Lapresté, "Dry camera calibration for underwater applications," *Machine Vision Applications,* vol. 13, nº 5-6, pp. 245-253, 2003.

[16] R. Eustice, O. Pizarro e H. Singh, "Visually augmented navigation for autonomous underwater vehicles," *Journal of Oceanic Engineering,,* vol. 33, nº 2, pp. 103-122, 2008.

[17] S. Negahdaripour, H. Sekkati e H. Pirsiavash, "Opti-acoustic stereo imaging: On system calibration and 3-d target reconstruction," *Transactions on Image Processing,* vol. 18, nº 6, pp. 1203-1214, 2009.

[18] T. Rahman, J. Anderson, P. Winger e N. Krouglicof, "Calibration of an underwater stereoscopic vision system," em *Oceans*, San Diego, USA, 2013.

[19] S. Ishibashi, "The study of the underwater camera model," em *Oceans*, Santander, Spain, 2011.

[20] J. Antich e A. Ortiz, "Underwater cable tracking by visual feedback," *Pattern Recognition and Image Analysis,* vol. 2652, pp. 53-61, 2003.

[21] M. Narimani, S. Nazem e M. Loueipour, "Robotics vision-based system for an underwater pipeline and cable tracker," em *Oceans*, Bremen, Germany, 2009.

[22] A. Ortiz, M. Simó e G. Oliver, "A vision system for an underwater cable tracker," *Machine vision and applications,* vol. 13, nº 3, pp. 129-140, 2002.

[23] T.-D. Zhang, W.-J. Zeng, L. Wan e Z.-B. Qin, "Vision-based system of auv for an underwater pipeline tracker," *China Ocean Engineering,* vol. 26, pp. 547-554, 2012.

[24] N. Otsu, "A threshold selection method from gray-level histograms," *Transactions on Systems, Man and Cybernetics,* vol. 9, nº 1, pp. 62-66, 1979.

[25] J. Bernsen., "Dynamic thresholding of grey-level images," em *International Conference on Pattern Recognition*, 1986.

[26] D. Bradley e G. Roth, "Adaptive thresholding using the integral image," *Journal of Graphics, GPU, and Game Tools,* vol. 12, nº 2, pp. 13-21, 2007.

[27] J. Sauvola e M. Pietikäinen, "Adaptive document image binarization," *Pattern Recognition,* vol. 33, nº 2, pp. 225-236, 2000.

[28] K. Chua e M. Rizal, "Robotics vision-based heuristic reasoning for underwater target tracking and navigation," em *Mobile Robots: towards New Applications*, A. Lazinica, Ed., InTech, 2006.

[29] M. An e C. Lee, "Stereo vision based on algebraic curves.," *Pattern Recognition,* vol. 1, pp. 476-482, 1996.

[30] R. Berthilsson, K. Åström e A. Heyden, "Reconstruction of general curves using factorization and bundle adjustment," *International Journal of Computer Vision,* vol. 41, nº 3, pp. 171-182, 2001.

[31] S. De Ma, "Conics-based stereo, motion estimation, and pose determination," *International Journal of Computer Vision,* vol. 10, nº 1, pp. 7-25, 1993.

[32] O. Faugeras e T. Papadopoulo, "A theory of the motion fields of curves," *International Journal of Computer Vision,* vol. 10, nº 2, pp. 125-156, 1993.

[33] J. Kaminski, M. Fryers, A. Shashua e M. Teicher, "Multiple view geometry of non-planar algebraic curves," em *International Conference on Computer Vision*, 2001.

[34] L. Quan, "Conic reconstruction and correspondence from two views," *Transactions on Pattern Analysis and Machine Intelligence,* vol. 18, nº 2, pp. 151-160, 1996.

[35] Y. Xiao e Y. Li, "Optimized stereo reconstruction of free-form space curves based on a nonuniform rational b-spline model," *Journal of the Optical Society of America A,* vol. 22, nº 9, pp. 1746-1762, 2005.

[36] D. E. B. Orozco, "Using epipolar geometry in stereo image analysis," Trieste, Italy, 2005.

[37] O. Faugeras, Three-dimensional Computer Vision: A Geometric Viewpoint, Cambridge, MA, USA: MIT Press, 1993.

[38] M. Moakher, "Means and averaging in the group of rotations," *Journal on Matrix Analysis and Applications,* vol. 24, nº 1, pp. 1-16, 2002.

[39] C. Tomasi e R. Manduchi, ""Bilateral filtering for gray and color images,"," em *Sixth International Conference on Computer Vision,*, 1998.

[40] E. H. Lockwood, A book of Curves, Cambridge University Press, 1973.

[41] "Orcina home of OrcaFlex," Orcina, [Online]. Available: http://www.orcina.com/index.php. [Acesso em july 2015].